Neuron, Vol. 46, 917–931, June 16, 2005, Copyright ©2005 by Elsevier Inc. DOI 10.1016/j.neuron.2005.05.018

NCAM 180 Acting via a Conserved C-Terminal Domain and MLCK Is Essential for Effective Transmission with Repetitive Stimulation

Luis Polo-Parada, Florian Plattner, Christian Bose, and Lynn T. Landmesser*
Department of Neurosciences
Case Western Reserve University School of Medicine
Cleveland, Ohio 44106

Summary

NCAM 180 isoform null neuromuscular junctions are unable to effectively mobilize and exocytose synaptic vesicles and thus exhibit periods of total transmission failure during high-frequency repetitive stimulation. We have identified a highly conserved C-terminal (KENESKA) domain on NCAM that is required to maintain effective transmission and demonstrate that it acts via a pathway involving MLCK and probably myosin light chain (MLC) and myosin II. By perfecting a method of introducing peptides into adult NMJs, we tested the hypothesized role of proteins in this pathway by competitive disruption of protein-protein interactions. The effects of KENESKA and other peptides on MLCK and MLC activation and on failures in both wild-type and NCAM 180 null junctions supported this pathway, and serine phosphorylation of KENESKA was critical. We propose that this pathway is required to replenish synaptic vesicles utilized during high levels of exocytosis by facilitating myosin-driven delivery of synaptic vesicles to active zones or their subsequent exocytosis.

Introduction

Adult mice that lack all three major isoforms of the neural cell adhesion molecule NCAM are unable to sustain effective transmission with high-frequency repetitive stimulation and exhibit both severe depression and total transmission failures. These mice also maintain an immature vesicle cycling mechanism in their axons and terminals (Polo-Parada et al., 2001). In contrast, mice that lack only the 180 kDa isoform of NCAM appropriately downregulate the immature vesicle cycling mechanism; however, transmission defects persist (Polo-Parada et al., 2004). While NCAM 180 null neuromuscular junctions (NMJs) do not exhibit severe depression, they do have periods of total transmission failures, with stimulus rates as low as 50 Hz. In addition, vesicle exocytosis is not selectively targeted to active zones apposed to muscle, and other presynaptic proteins are more diffusely localized, including the P/Q-type Ca^{2+} channels responsible for transmission at these NMJs (Polo-Parada et al., 2004).

How might the absence of the 180 kDa isoform of NCAM result in these severe defects in presynaptic structure and function? NCAM participates in developmental events, including axon growth and fasciculation, cell migration, and synaptic maturation (Rutishauser and Landmesser, 1996; Kiss and Muller, 2001). Of the three major alternatively spliced isoforms, the 120 kDa isoform is GPI linked, whereas the 140 and 180 kDa isoforms are transmembrane proteins, with cytoplasmic portions of different lengths (Cunningham et al., 1987; Barbas et al., 1988). The extracellular portion of NCAM, which is essentially identical for all isoforms, can mediate homophilic interactions with itself or heterophilic interactions with other molecules (for reviews, see Panicker et al., 2003; Hinsby et al., 2004). In addition to adhesion per se, NCAM has also been shown to activate several intracellular signaling cascades (for reviews, see Crossin and Krushel 2000; Panicker et al., 2003; Hinsby et al., 2004). Upon clustering of NCAM 140, the tyrosine kinase fyn is activated, stimulating the MAP-kinase pathway (Schmid et al., 1999; Kolkova et al., 2001). Interaction of NCAM 140 with the FGF receptor evokes a signaling cascade via phospholipase C and DAG, which leads to the influx of Ca^{2+} (Safell et al., 1997). Both of these signaling cascades enhance neurite extension.

The recently described defects in transmission at NCAM 180 null adult NMJs (Polo-Parada et al., 2004) suggest that, rather than acting as a homophilic adhesion molecule, the 180 isoform of NCAM may act via signaling or direct protein-protein interactions to organize presynaptic release machinery that is required to sustain effective transmission with repetitive stimulation. This prompted us to undertake a bioinformatical characterization of the intracellular domain of NCAM. Multiple potential interaction sites were detected within the cytosolic portion of NCAM, including a domain at the extreme C terminus of both 140 and 180 kDa isoforms that resembles a class I PDZ binding motif. We chose to focus our studies on this domain since such motifs have been shown to mediate the formation of macromolecular complexes both pre- and postsynaptically that are required for effective synaptic transmission (Craven and Bredt, 1998; Kim and Sheng, 2004). Furthermore, the conservation of this C terminus domain in NCAM homologs and orthologs across many species suggested that it was mediating a critical function.

To probe the function of this domain in transmission at adult mouse NMJs, we adapted a commercially available peptide carrier (see Experimental Procedures) system to introduce the heptapeptide KENESKA, representing the C-terminal portion of this conserved domain, into adult NMJs. We then assessed the acute effect on functional transmission and demonstrate here that the cyclical total transmission failures that occur in 180 null NMJs with repetitive stimulation are phenocopied by the introduction of this peptide and, further, that serine phosphorylation of this domain is critical. In addition, we show that myosin light chain kinase (MLCK) is a probable target of the NCAM-mediated signaling and/or protein interactions mediated by this domain. We speculate that sufficient MLCK activity following repetitive stimulation may be required to convey and/or exocytose synaptic vesicles at sufficient rates to

*Correspondence: lynn.landmesser@case.edu

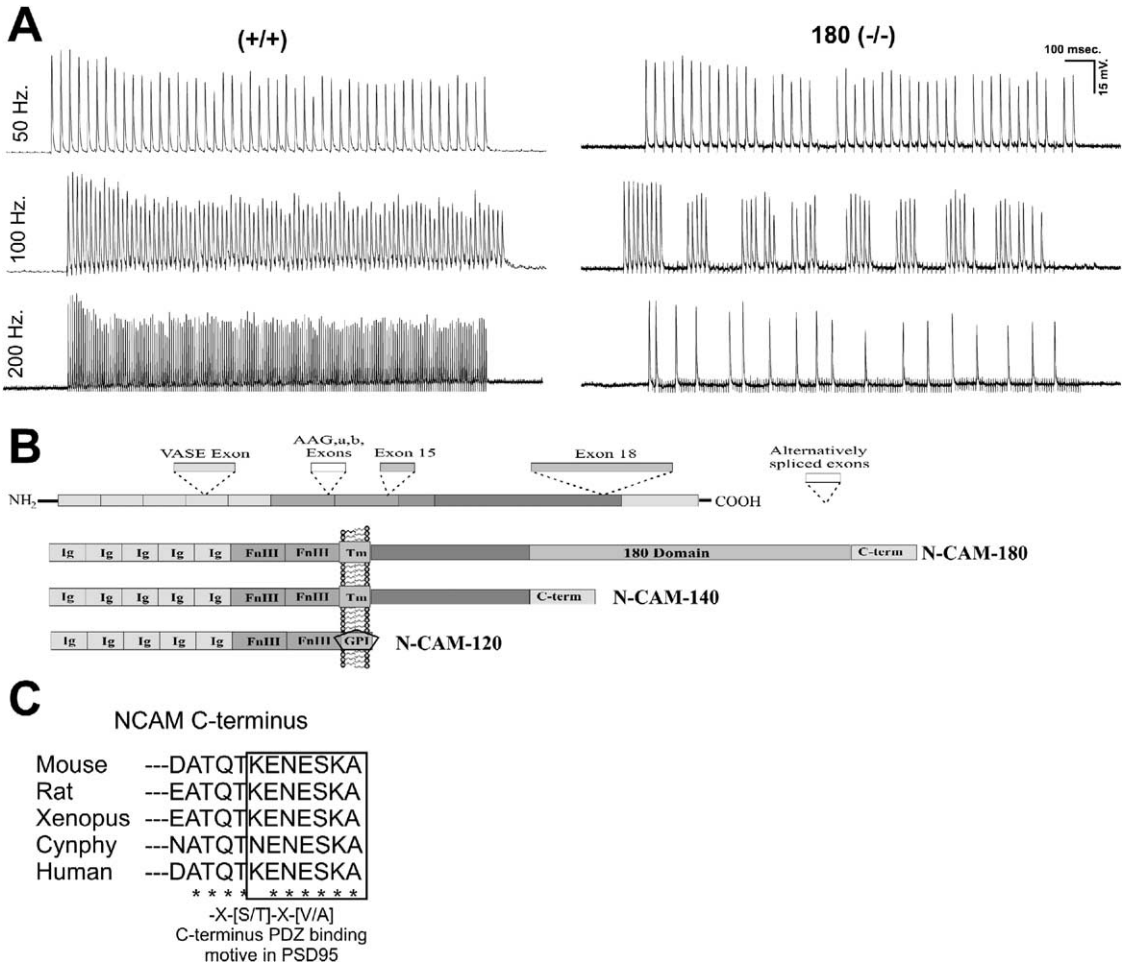

Figure 1. Transmission Defects in the NCAM 180 Isoform Null NMJ and the Domain Structures of the Three Major NCAM Isoforms

(A) Wild-type P30 mouse NMJs do not exhibit transmission failures when stimulated with high-frequency trains, whereas NMJs lacking the 180 isoform of NCAM exhibit bouts of complete transmission failures.

(B) Overall domain structure of the alternatively spliced isoforms of NCAM.

(C) The C-terminal domain, which is highly conserved across species (data shown for mouse, rat, *Xenopus*, salamander, and human) contains a PDZ-like binding motif and a putative serine phosphorylation site and is present in both the 140 and 180 isoforms of NCAM.

maintain effective transmission, probably via myosin-driven vesicle movement or other cytoskeletal alterations.

Results

Inability of NMJs Lacking All Isoforms or Only the 180 kDa Isoform of NCAM to Sustain Transmission with High-Frequency Repetitive Stimulation

Wild-type adult mouse NMJs are capable of sustaining effective transmission even when stimulated at frequencies as high as 200 Hz (Figure 1A). This requires extensive synaptic vesicle cycling, since each EPP is composed of approximately 90–100 quanta or vesicles. Mice lacking only the 180 kDa isoform of NCAM do not exhibit the severe depression previously observed in the NCAM null NMJs (Polo-Parada et al., 2001), but do exhibit cyclical periods of total transmission failures at stimulation frequencies of 50 Hz and above (Figure 1A; Polo-Parada et al., 2004).

Our previous studies (Polo-Parada et al., 2001; Polo-Parada et al., 2004) suggested that NCAM might contribute to effective high-frequency repetitive transmission by helping to organize the presynaptic molecular machinery required to sustain such high-demand synaptic vesicle cycling. Since this seemed likely to involve NCAM participating in intracellular signaling cascades or perhaps in a scaffold with other molecules required for high-frequency transmitter release and synaptic vesicle cycling, we carried out a bioinformatic characterization of the intracellular domain of NCAM.

A Bioinformatic Analysis of the Intracellular Domain of NCAM Reveals a Highly Conserved C-Terminal Domain with a PDZ-like Binding Motif and a Putative Serine Phosphorylation Site

The amino acid sequence of NCAM is highly conserved among vertebrate species, as is the overall domain organization (Figure 1B, top). While the 140 and 180 kDa isoforms share highly homologous transmembrane and

extracellular domains, the 180 kDa isoform contains an additional 267 amino acid long alternatively spliced insert (residue 810–1076) encoded by exon 18 (Cunningham et al., 1987), and its sequence varies more between species. The cytoplasmic sequence of NCAM has a high content of hydrophilic (50%), charged (21%), and proline (14%) residues, the latter being observed in many synaptic proteins (Kay et al., 2000). Few secondary structures, such as α-helix, β sheet, or random coil, would be predicted within the cytoplasmic tail due to the high content of proline and charged hydrophilic residues. This implies that the cytoplasmic domain has an extended, exposed structure that could provide multiple protein interaction sites. Within the 180-specific domain, we identified several sequences (871–893, 930–970) with high similarities to cytoskeleton binding proteins. Indeed, a recent study has reported interactions of the NCAM 180 isoform with β-actin, tropomyosin, and microtubule-associated protein MAP 1A (Buttner et al., 2003). Such cytoskeletal interactions might constrain the molecule within the synapse and account for the punctate immunostaining of the NCAM 180 isoform at junctions (Polo-Parada et al., 2004).

The carboxy-terminal sequence of NCAM (ATQTKEN ESKA) is conserved across diverse species (Figure 1B, bottom), and the most C-terminal portion KENESKA resembles a class I PDZ binding domain. PDZ domains are found in numerous scaffolding/adaptor molecules such as PSD-95 and Discs-large (Dg) (Kim and Sheng, 2004) where they mediate the clustering and localization of interacting proteins at specific synaptic sites (Craven and Bredt, 1998; Kim and Sheng, 2004). Furthermore, it has been demonstrated that functions/interactions of the PDZ domain are regulated via phosphorylation of the serine/threonine residues within the sequence (Chung et al., 2004; Kim and Sheng, 2004). The high degree of conservation of this PDZ domain indicated its likely importance in NCAM's function. It further suggested that interactions between this domain and other molecules in the presynaptic terminal might serve to target other molecules to specific sites, bringing about the appropriate targeting of transmitter release to precise active zones as well as facilitating the delivery of synaptic vesicles to these zones; both of these processes appear to be defective in the 180 isoform null NMJ (Polo-Parada et al., 2004).

Adaptation of a Peptide Carrier to Acutely Introduce Peptides into Adult NMJs to Assess the Role of Particular Molecular Domains on Specific Aspects of Functional Transmission

The adult NMJ is a complex structure, consisting of highly organized and aligned pre- and postsynaptic macromolecular aggregates and includes the presynaptic terminal, an extensive synaptic basal lamina, the postsynaptic muscle cell with extensive junctional folds, as well as specialized Schwann cells that cap the nerve terminal. It arises through a complex series of bidirectional developmental interactions (Sanes and Lichtman, 1999). Junctions formed in culture, while amenable to viral transfection and electroporation, do not contain all the components of the adult in vivo NMJ. Furthermore, while direct protein-protein interactions can be detected by yeast two-hybrid assays, direct introduction of peptides that can block specific interactions into the adult NMJ allow one to assess their impact on multiple aspects of mature functional transmission in a physiologically intact setting. In addition, the introduction of phosphopeptides would allow one to probe the importance of the phosphorylation state of various proteins in mediating specific effects. We therefore surveyed several methods based on the Tat or antennapedia means of getting peptides into cells (Kabouridis, 2003) and found that a commercially available product, Chariot (Active Motif, Carslbad, CA), allowed us to effectively introduce peptides into adult NMJs.

Following dissection of semitendinosus muscles from adult wild-type P30–P40 mice, an extensive electrophysiological characterization of functional transmission was carried out at physiological Ca^{2+} levels according to previously described protocols (Polo-Parada et al., 2004). This included an analysis of EPP amplitude, MEPP frequency and amplitude, and the ability of NMJs to sustain transmission when stimulated with 1 s trains at frequencies of 10, 20, 50, 100, and 200 Hz. The peptide carrier alone was then applied for 1 hr while recording from a muscle fiber. Following washout of the carrier from the bath, the functional analysis of transmission was repeated. When the peptide carrier alone was applied at several different concentrations, we detected no changes in muscle resting potential or an increase in MEPP frequency that might indicate a presynaptic depolarization during the 1 hr application. Following washout of the carrier, we also detected no changes in any parameter of transmission compared to either precarrier measurements or data from other wild-type junctions (Figure 2A). There were no alterations in the ability of the junction to sustain transmission when stimulated with 50, 100, and 200 Hz 0.5–1 s trains during the period tested (several hours) (Figure 2B). We therefore combined the carrier with specific peptides, according to the manufacturer's instructions, and applied these to adult, acutely dissected NMJs for 1 hr, determining their effects on transmission after washout of carrier/peptide from the bath.

Introduction of the NCAM KENESKA Peptide into Wild-Type NMJs Results in Transmission Failures at High Stimulation Rates and Its Effectiveness Is Modulated by Serine Phosphorylation

When the KENESKA peptide with carrier was introduced into P30 wild-type NMJs using a bath concentration of 3 μM for 1 hr and then washed out, electrophysiological analysis revealed no changes in quantal content, MEPP frequency or size, or depression in response to trains of stimuli (Figure 3A). However, when the junctions were stimulated with repetitive stimulation, transmission failures became apparent at 100 Hz and increased at 200 Hz (Figures 3B and 3C, left panels). When the concentration of the peptide was reduced 10-fold to 0.3 μM, there were no transmission failures, although some depression was apparent. For each concentration, the number of failures or lack thereof per 100 Hz train remained constant over several hours (0.3 μg, no failures; 3 μg, 38 ± 5 failures; 300 μg, 42 ± 7 failures; n = 8). These observations suggest that the experiments presented in this study were carried

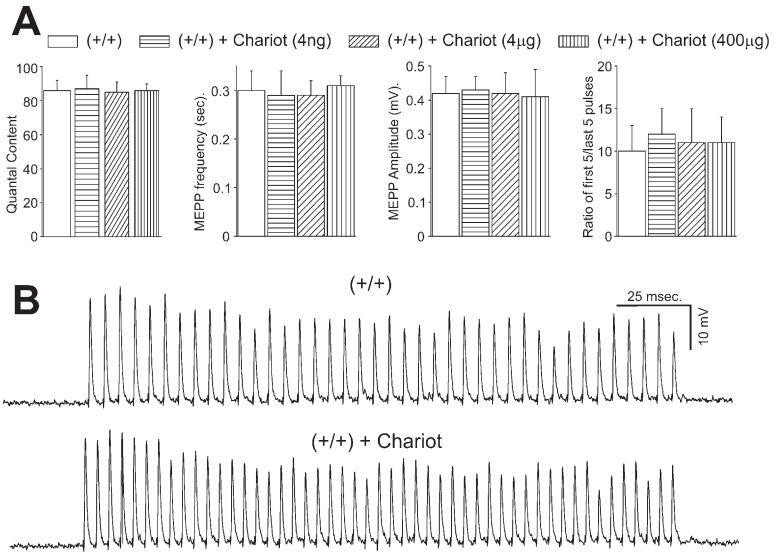

Figure 2. The Peptide Carrier Chariot Does Not Produce Any Alterations in Transmission at Wild-Type NMJs

(A) Exposure of P30 wild-type NMJs to Chariot alone for 30 min at three different concentrations had no effect on the quantal content, MEPP frequency or amplitude, or depression (expressed as the ratio of the mean EPP amplitude of the first five to the last five stimuli in a 1 s train).

(B) Introduction of Chariot alone also did not result in any transmission failures at any stimulation frequency, including 200 Hz, as shown by traces of EPPs recorded in 2 mM Ca^{2+} solution.

Quantification of data is expressed as the mean ± SEM.

out at concentrations in an appropriate part of the dose-response curve (3 μg for KENESKA) and that they were therefore likely to be in the physiological range. The fact that such failures were only found at high stimulus repetition rates but that all transmission parameters were normal to single stimuli showed that the overall health of the junctions was maintained and that basic exo- and endocytosis of vesicles was occurring normally. As in the 180 null NMJs, defects only became apparent when junctions were challenged at high stimulus repetition rates. Previously we found that introduction of the larger NCAM-derived ATQTKENESKA peptide produced similar results as the KENESKA peptide (data not shown).

The KENESKA domain has a putative serine phosphorylation site, although the kinases that might phosphorylate this site in vivo are unknown. To assess whether the phosphorylation of this site affected the ability of the peptide to alter high-frequency transmission, a peptide in which this serine had been phosphorylated was introduced into wild-type junctions. As shown in Figures 3B and 3C (middle panels), the phosphorylated peptide produced a larger number of failures, and these were more cyclic and occurred at lower stimulus repetition rates than when the nonphosphorylated peptide was introduced. Overall, this phenotype more closely resembled the phenotype in the 180 null NMJ (compare Figures 3B and 3C, middle panels, to Figure 1A). Replacement of the serine with an aspartate, which should mimic phosphorylation of this site, produced a similar amount of transmission failures (Figure 3B, right panel) as did the phosphorylated KEN ESKA peptide. However, when the serine was replaced by a glycine (KENEGKA), which is unable to be phosphorylated, there was no effect on transmission even at 200 Hz (Figure 3C, right panel). This result also served as a control for nonspecific effects of the introduced peptide. In addition, introduction of a scrambled peptide, CSNKATAETKQE, also was without effect (data not shown).

Taken together the data strongly suggest a specific effect of the KENESKA domain on NCAM in sustaining effective high-frequency transmission and that serine phosphorylation is critical. None of the introduced peptides had any effects on basic transmission parameters to single stimuli (Figure 3A). We propose that introduction of the exogenous KENESKA peptide into the junction interferes with the normal function/protein interactions of the KENESKA domain on NCAM and thus mimics the transmission defects when this domain is lacking in either the NCAM null or 180 isoform-specific null NMJ.

The unusual total transmission failures could occur if there were intermittent branch point failures in the conduction of action potentials with resultant failure of the presynaptic terminals to be depolarized. Since mouse NMJs are not actively invaded by the action potential but electrotonically depolarized by currents from the last node or hemi-node, it is possible to record the various currents, including that of Ca^{2+} influx in the terminal, by extracellular epineural recordings (Brigant and Mallart, 1982). We have previously found that in NCAM 180 null NMJs, there were no alterations in Na^+, K^+, or Ca^{2+} currents with high-frequency repetitive stimulation that would indicate failures of the nerve terminal to be depolarized or a reduction in Ca^{2+} influx (Polo-Parada et al., 2004). To exclude the possibility that introduction of the KENESKA peptide produced transmission failures by affecting nerve terminal depolarization or Ca^{2+} influx, we repeated these recordings on KENESKA-treated wild-type NMJs. Following the stimulus artifact, a fast sodium and slower potassium current were recorded (Figure 3D, arrows). During a 100 Hz train, during which multiple total transmission failures were always detected in the KENESKA-treated terminal (Figures 3B and 3C), there were no alterations in these currents (Figure 3F). When the Ca^{2+}-activated K^+ current was blocked with 3,4-diaminopyridine, a peak that represents the Ca^{2+} current and which was completely blocked by cadmium (data not shown) was revealed (Figure 3E, arrow; see also Polo-Parada et al., 2004, Figure 5). Although there were slight fluctuations in the size of this current during a 100 Hz train, there were no large reductions (Figure 3G) that could account

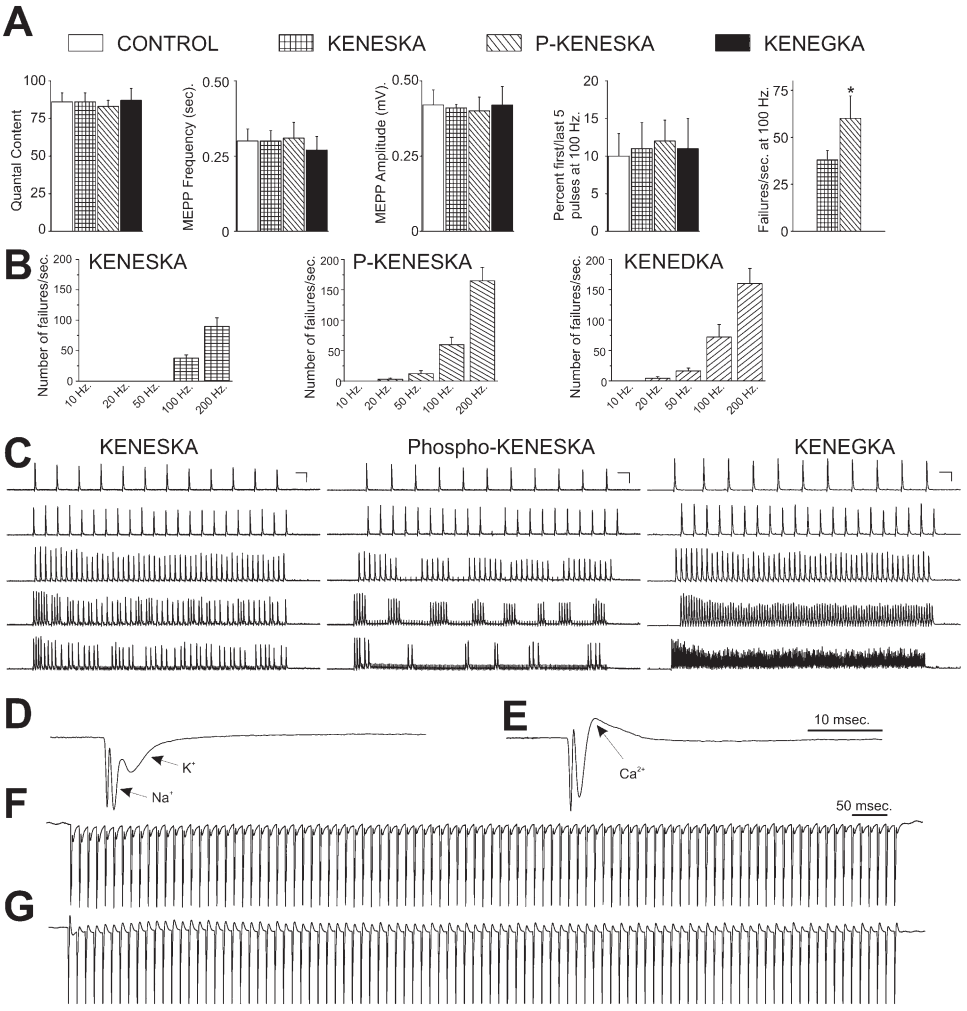

Figure 3. Effect of KENESKA, Phospho-KENESKA, and Control Peptides on Transmission at P30 Wild-Type NMJs

(A) Introduction of KENESKA, phospho-KENESKA, or the control KENEGKA via the Chariot peptide carrier into wild-type NMJs did not alter quantal content, MEPP frequency, MEPP amplitude, or depression (expressed as the ratio of the mean EPP amplitude of the first five to the last five stimuli in a 1 s train) compared to controls (white bars).

(B) However, failures at 100 Hz stimulation were produced by KENESKA and to a greater extent by phospho-KENESKA and KENEDKA, which mimics phosphorylation of serine at this site. Bar graphs of the number of failures produced by KENESKA (left bar graph), phospho-KENESKA (middle bar graph), and KENEDKA (right bar graph) at different stimulation frequencies. No failures were produced by the control KENEGKA peptide at any frequency.

(C) Example traces of EPPs in response to 10, 20, 50, 100, and 200 Hz stimulation following introduction of KENESKA (left panel), phospho-KENESKA (middle panel), and KENEGKA (right panel).

(D–G) Extracellular epineural recordings of the Na^+, K^+, and Ca^{2+} currents from wild-type NMJs treated with the KENESKA peptide. (D) The response to a single stimulus reveals a fast Na^+ current and a slower K^+ current (arrows) following the stimulus artifact. When a 100 Hz train was applied (F), there were no reductions in these currents that would indicate a failure of the nerve terminal to be depolarized. (E) Treatment with 100 μM 3,4-diaminopyridine to block Ca^{2+}-activated K^+ current revealed a slower peak that was completely blocked by 200 μM cadmium (data not shown) and which thus represents the Ca^{2+} influx into the terminal. (G) There was no reduction or complete block of this current during a 100 Hz train that would indicate a failure of Ca^{2+} influx as underlying the total transmission failures observed as in Figure 3C, left panel.

Quantification of data is expressed as the mean ± SEM.

for the total transmission failures produced by the KEN ESKA peptide. Thus, as with the failures at the NCAM 180 null NMJs, we propose that these failures are produced by a mechanism downstream of nerve terminal depolarization and Ca^{2+} influx.

The KENESKA Domain of NCAM May Mediate Its Effect on Transmission through Downstream Activation of Myosin Light Chain Kinase

We previously observed that transmission failures similar to those observed in NCAM null or 180 isoform null NMJs could be produced by the MLCK inhibitor ML-9 at concentrations considered specific for MLCK (Polo-Parada et al., 2001; Polo-Parada et al., 2004). Previous studies have shown that inhibiting the action of MLCK by drugs such as ML-9 (Ryan, 1999) or specific blocking peptides (Mochida et al., 1994; Mochida, 1995) interferes with normal neural transmission. However, because of potential lack of specificity of ML-9, we used the peptide carrier method to introduce an inhibitory peptide known to block MLCK (Kemp et al., 1987). Five major alternatively spliced isoforms of MLCK are

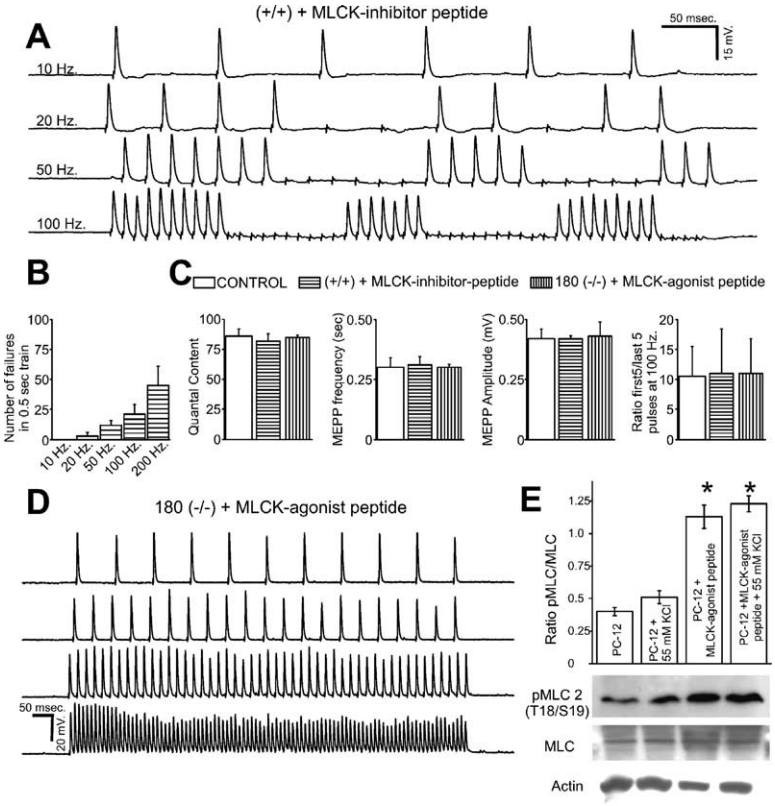

Figure 4. The Effect of Peptides that Inhibit or Make MLCK Constitutively Active on Transmission at Wild-Type P30 and NCAM 180 Null NMJs

(A) The MLCK inhibitory peptide at a bath concentration of 3 μM was introduced into a wild-type NMJ that was then stimulated at 10, 20, 50, and 100 Hz. The EPP traces show that transmission failures were apparent at 20 Hz and became more pronounced at higher stimulation frequencies.

(B) The number of failures in a 0.5 s train at each of these frequencies is quantified for multiple junctions (n = 12).

(C) Bar graphs showing quantal content, MEPP frequency, MEPP amplitude, and depression (expressed as the ratio of the mean EPP amplitude of the first five to the last five stimuli in a 1 s train) in control wild-type, wild-type with MLCK inhibitory peptide, and NCAM 180 null NMJs with the MLCK agonist peptide.

(D) Introduction of the MLCK agonist peptide into a NCAM 180 null NMJ at a bath concentration of 3 μM rescued the transmission failures when stimulus trains of 10, 20, 50, and 100 Hz were applied for 0.5 s.

(E) (Top) Bar graphs quantifying the level of myosin light chain phosphorylation via the ratio of immunostaining with an antibody that recognizes MLC when it is phosphorylated at threonine 18/serine 19 over immunostaining with a pan MLC antibody in PC12 cell lysates, made from PC12 cells that were either untreated or assayed 5 min following an exposure to 55 mM KCl for 1 min or assayed following the introduction of the MLCK agonist peptide with or without KCl-mediated depolarization (the latter two treatments resulted in a significant increase in phosphorylated MLC versus the control; $p < 0.05$). (Bottom) A representative Western blot showing the bands for phosphorylated MLC, all MLC, and actin as a loading control under these same conditions. Quantification of data is expressed as the mean ± SEM.

known (Kamm and Stull 2001), including a "smooth muscle isoform" and a "nonmuscle isoform." The smooth muscle isoform has been studied extensively since it is a major regulator of smooth muscle contraction. The inhibitory peptides mimic the binding of an autoinhibitory domain of MLCK to prevent MLCK activation. Following stimulation of neurons or muscle there is a Ca^{2+}/calmodulin activation of MLCK, resulting in a conformational change, allowing MLCK to phosphorylate myosin light chain (Kamm and Stull, 2001). We found that a MLCK inhibitory peptide (see Experimental Procedures) caused periods of transmission failures that closely resembled those of the 180 null NMJ. Transmission failures were common even at 50 Hz and became even more frequent at 100 Hz (Figures 4A and 4B). The MLCK inhibitory peptide had no effect on quantal content, MEPP frequency or amplitude, or depression (Figure 4C). Thus, as with the KENESKA peptide, failures in transmission were only detected with repetitive stimulation.

These results suggest that transmission may be impaired at junctions that lack all or only the 180 isoform of NCAM, because MLCK is not appropriately activated. If true, one would predict that constitutively activating MLCK would rescue the transmission defects in NMJs that lack NCAM. Indeed, when we introduced a peptide that we designed to interact with MLCK, inducing a conformation to make MLCK constitutively active (see Experimental Procedures) into NCAM null (data not shown) or 180 isoform null NMJs (Figure 4D), the transmission failures observed at high stimulus rates were completely prevented. To ensure that our designed peptide constitutively activated MLCK, we tested its ability to lead to phosphorylation of myosin light chain (MLC) in the absence of stimulation.

To obtain sufficient material for biochemical analysis, we used cultures of PC12 cells that had been stimulated to differentiate into a neuronal form. These cells were either not stimulated or stimulated with exposure to high K^+ (55 mM) for 1 min. Following stimulation, MLCK-mediated phosphorylation of serine 19 and threonine 18 on MLC is generally considered to peak within seconds and to then decline toward baseline within minutes (Somlyo and Somlyo, 2003). We therefore performed Western blots of the PC12 cell lysates at 5 min after stimulation using an antibody that specifically recognizes serine 19 and threonine 18 on MLC when they are phosphorylated. Figure 4E shows that there is a baseline level of phosphorylation that occurs even in the unstimulated cells (lane 1). Five minutes following the 55 mM K^+ stimulation, phosphorylation was still somewhat increased over the baseline values (lane 2). However, introduction of the peptide to make MLCK constitutively active resulted in a 3-fold increase in phosphorylation in both the unstimulated and stimulated cells (lanes 3 and 4, respectively). There was no

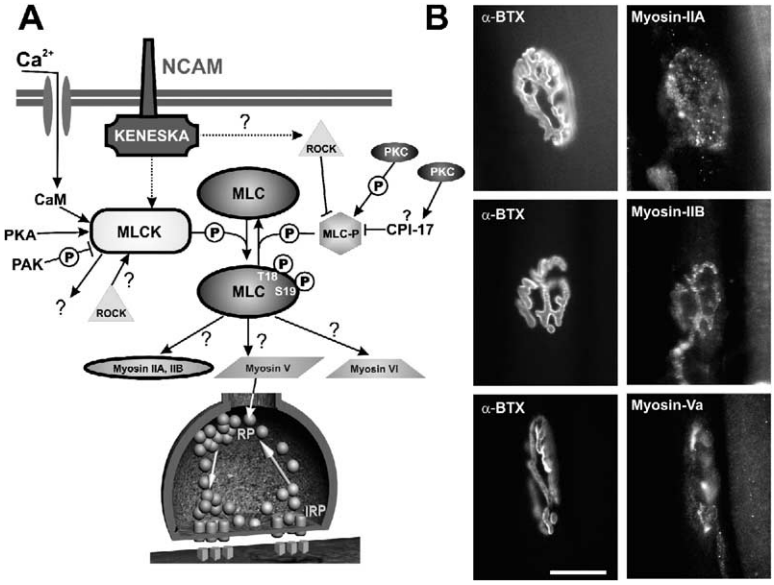

Figure 5. Major Pathways by which the KENESKA Domain of NCAM May Affect Transmission by Altering MLCK and MLC Activation

(A) Diagram showing that the major target of MLCK is its phosphorylation of MLC at serine 19/threonine 18. The level of phosphorylation at this site depends on the balance of MLC kinase and MLC phosphatase. Rho kinase, PKC, and PKA can also potentially modulate this pathway. Outlined in bold are the molecules that our data support as being in the pathway required for sustained transmission at high stimulus frequencies.

(B) Immunostaining of wild-type NMJs show that myosin IIA, myosin IIB, and myosin Va are all present at P30 wild-type endplates (right panels), visualized by the α-BTX staining (left panels). Immunostaining for these myosins also occurred to some extent along preterminal axons (see, for example, that of myosin IIB). Calibration bar, 40 μM.

Quantification of data is expressed as the mean ± SEM.

change in the level of MLC, visualized with a pan-MLC antibody that recognizes both phosphorylated and nonphosphorylated states, nor in the level of actin used as a loading control. In summary, the peptide that we have designed does appear to make MLCK constitutively active, even in the absence of stimulation and Ca^{2+}/calmodulin activation. The fact that this peptide rescued the transmission failures in NCAM 180 null NMJs strongly suggests that inadequate activation of MLCK occurs in the absence of the 180 isoform of NCAM and that this underlies the transmission failures.

The data presented thus far indicate that MLCK is an important link in the pathway by which the KENESKA peptide, and by inference this domain on NCAM, allows mouse NMJs to maintain a high level of transmitter output, even when challenged by high-frequency stimulation. Although MLCK may have other targets, its most generally accepted role is in the activation of myosin light chain via phosphorylation of serine 19 and to a lesser extent threonine 18. This in turn stimulates actin binding and filament formation by myosin II heavy chain, which increases the MHC ATPase activity necessary for force generation (Somlyo and Somlyo, 2003). Figure 5A illustrates the major pathways known to regulate phosphorylation of serine 19 and threonine 18 in other systems and shows that its activation is a balance between phosphorylation by MLCK and dephosphorylation by myosin light chain phosphatase (MLC-P) (Isotani et al., 2004; see Brown and Bridgman, 2003, Somlyo and Somlyo, 2003, and Riento and Ridley, 2003, for reviews). Many signal transduction pathways can affect both MLCK and MLC-P activity, including PKA, PKC, Ca^{2+}-CaM, and Rho kinases. Various studies have provided evidence for a role of several myosins, such as myosin IIA, IIB, and V, in the movement of vesicles and in secretion (Rose et al., 2003; Neco et al., 2004; Libby et al., 2004), although the cellular mechanisms are not well understood and their roles may differ with cell type. We have previously demonstrated that MLCK is highly expressed at wild-type, NCAM null, and NCAM 180 null NMJs (Polo-Parada et al., 2004). Figure 5B shows that mouse NMJs also express myosin IIA, myosin IIB, and myosin Va. In the experiments described below, we have attempted to use peptide and other specific inhibitors, alone or in combination, to begin to elucidate the pathways underlying the transmission failures that result from the lack of the 180 isoform of NCAM.

The KENESKA Peptide Appears to Be Mediating Effects on Transmission Primarily through Its Effect on MLCK

If the lack of NCAM or the 180 isoform of NCAM is producing transmission failures solely because of the inability of the KENESKA domain of the 180 kDa isoform of NCAM to interact with other presynaptic proteins, one would predict that introduction of this peptide into the NCAM mutant junctions should not produce effects on transmission additive to those brought about by the absence of the NCAM 180 itself. As shown in Figure 6A, introduction of the peptide into the NCAM 180 null NMJs did not produce additional failures in transmission compared to the mutant phenotype. Similar results were found when KENESKA was introduced into the total NCAM null NMJ (data not shown). Introduction of the phosphorylated KENESKA peptide also did not produce additional transmission failures.

Similar reasoning would suggest that, if the KEN ESKA peptide is producing its effect on transmission solely by preventing the full activation of MLCK, making MLCK constitutively active should abrogate the transmission failures produced by the introduction of the KENESKA peptide. Indeed, when the MLCK agonist peptide was introduced into a wild-type NMJ 30 min prior to introduction of the KENESKA peptide, no transmission failures were produced (Figure 6B). To ensure that the KENESKA peptide, when applied sequentially after application of the MLCK agonist peptide, was actually entering the cell, the following control experiment was performed. The KENEGA peptide, which had pro-

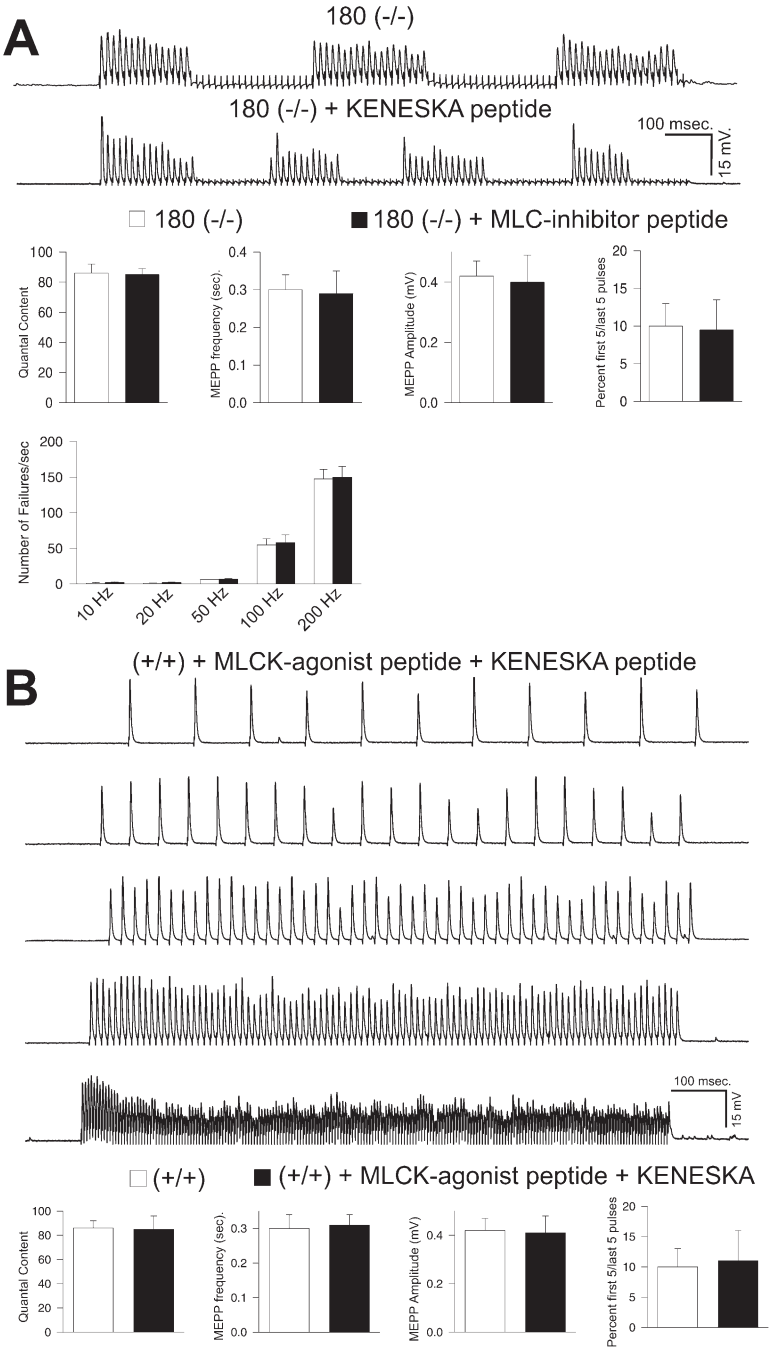

Figure 6. Effects of the KENESKA Peptide on NCAM 180 Null NMJs and on Wild-Type NMJs in which MLCK Has Been Made Constitutively Active

(A) (Top) Traces showing an example of EPPs in response to a 100 Hz train in a 180 null NMJ (top trace) and a 180 null NMJ into which the KENESKA peptide was introduced (bottom trace). (Middle) Bar graphs showing that introduction of the KENESKA peptide into 180 null NMJs (black bars) does not alter quantal content, MEPP amplitude, MEPP frequency, or depression, compared to untreated NCAM 180 null NMJs. (Bottom) The number of failures within 1 s trains of stimuli for NCAM 180 null NMJs (white bars) and 180 null NMJs treated with the KENESKA peptide (black bars) did not differ significantly ($p < 0.05$) for 10, 20, 50, 100, or 200 Hz stimulation.

(B) No effects on transmission are produced by the KENESKA peptide when introduced into wild-type NMJs in which the MLCK agonist peptide had been introduced 30 min before. (Top) Examples of EPPs during 0.5 s trains at 10, 20, 50, 100, and 200 Hz. (Bottom) Bar graphs showing the effect of this dual treatment (black bars) on quantal content, MEPP amplitude, MEPP frequency, and depression compared to wild-type NMJs (white bars).

duced no failures when applied alone, was applied first. As expected, no failures were produced, but the subsequent application of the KENESKA peptide resulted in 45 ± 11 (n = 7) failures during a 100 Hz train, which was not significantly different from 38 ± 5 failures that had been found previously when KENESKA was applied alone. Taken together these observations provide evidence that the effect of the KENESKA peptide, and thus we infer of this domain of NCAM, in preventing transmission failures with high-frequency repetitive stimulation, is mediated primarily through MLCK.

The Effects of MLCK on Transmission May Be Mediated by Its Phosphorylation of Myosin Light Chain

As noted earlier, MLCK regulates MLC via phosphorylation of serine 19/threonine 18. Figure 7A (top left pair) shows that an antibody that recognizes MLC when both of these residues are phosphorylated causes strong punctate immunostaining in control wild-type NMJs. Furthermore, such immunostaining was greatly decreased in NMJs into which the KENESKA peptide had been introduced 1 hr before (top right pair). Quan-

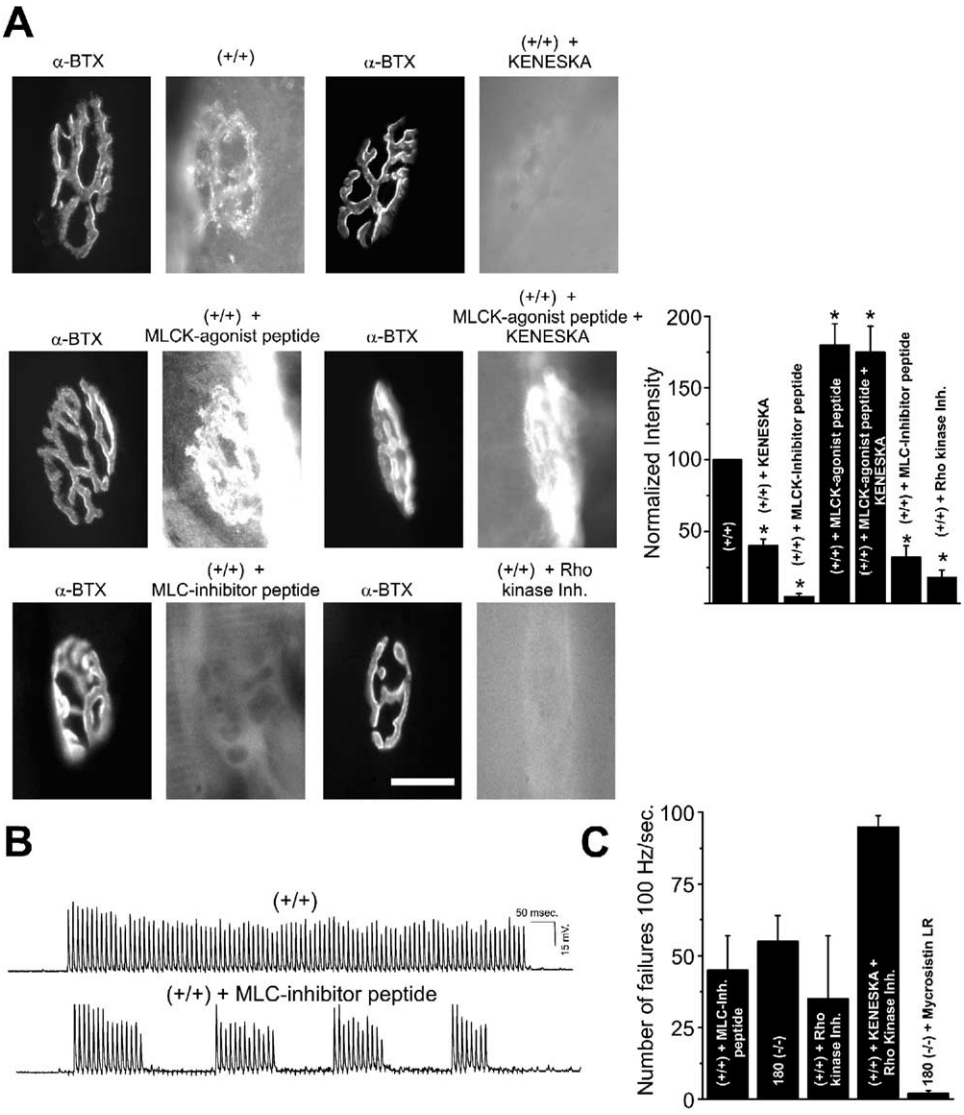

Figure 7. Changes in MLC Phosphorylation by Peptides that Altered the Ability of NMJs to Maintain Effective Transmission with Repetitive Stimulation

(A) Immunostaining of P30 NMJs with an antibody that recognizes MLC only when serine 19 and threonine 18 are phosphorylated shows bright punctate staining at endplates visualized by α-Btx (top left pair). Introduction of the KENESKA peptide greatly reduced this staining (top right pair). In contrast, introduction of the MLCK agonist peptide greatly increased the immunostaining at the endplate (middle left pair). Prior introduction of the MLCK agonist peptide prevented the reduction in immunostaining caused by the KENESKA peptide (middle right pair). The MLC inhibitor peptide (bottom left pair) and the Rho kinase inhibitor Y2362 (bottom right pair) also reduced immunostaining for phospho-MLC. Bar graph at far right shows quantification of immunostaining of different peptides/inhibitors when applied alone or in combination (see Experimental Procedures and Polo-Parada et al., 2004, for details).

(B) Introduction of a MLC inhibitory peptide produced transmission failures in a P30 NMJ stimulated at 200 Hz.

(C) Bar graph showing the number of failures/s during a 100 Hz train for the MLC inhibitor peptide and the Rho kinase inhibitor Y2362 at 100 μM at wild-type NMJs compared to the failures in the NCAM 180 null NMJs and the phosphatase inhibitor microcystin-LR at 10 μM at 180 null NMJs.

Quantification of data is expressed as the mean ± SEM.

tification of the phospho-MLC immunostaining (bar graph, right) showed that the reduction in immunostaining was statistically significant. Phospho-MLC levels were also reduced by the MLCK inhibitory peptide (bar graph, right). In contrast, introduction of the peptide, which was demonstrated to make MLCK constitutively active in PC12 cells (Figure 4E), caused a large increase in phospho-MLC in the endplate (Figure 7A, middle left pair and bar graph). It also increased phospho-MLC immunostaining in muscle fibers and in smooth muscle of intramuscular blood vessels (data not shown). Finally, introduction of the KENESKA pep-

tide into NMJs in which MLCK had been made constitutively active did not reduce immunostaining for phospho-MLC (middle right pair and bar graph). Taken together, the observations obtained with the phospho-specific MLC antibody provide evidence that the KEN ESKA peptide results in alterations in the level of serine19/threonine 18 phosphorylation that are consistent with the proposed role of this domain of NCAM in synaptic transmission.

Additional evidence that failure of this site on MLC to be phosphorylated leads to transmission failures was obtained by introducing a peptide (MLC inhibitory peptide, see Experimental Procedures) that mimics this site and that should therefore compete for phosphorylation of this site on MLC by MLCK and thus prevent or reduce its phosphorylation. Failures in transmission at high frequencies, at the approximate level of those caused by phospho-KENESKA, were in fact produced when this peptide was introduced into wild-type NMJs (Figures 7B and 7C), while other parameters of transmission, including MEPP amplitude, frequency, and quantal content to single stimuli, were not altered (data not shown). This peptide also reduced the level of immunostaining for phospho-MLC (Figure 7A, bottom left pair and bar graph).

In other systems, Rho kinase has been shown to indirectly result in phosphorylation of MLC. While this can occur via several routes (see Figure 5), the most generally accepted one is by Rho kinase inhibiting MLC-P, which in turn results in higher levels of MLC phosphorylation (Isotani et al., 2004; Somlyo and Somlyo, 2003; Riento and Ridley, 2003). Furthermore, it has been reported that the 180 but not the 140 cytoplsmic domain of NCAM, when used in affinity column chromatography, is able to pull down Rho kinase (Buttner et al., 2003). The Rho kinase inhibitor Y-27632, which strongly inhibits phosphorylation of this site in retinal ganglion cells (Wahl et al., 2000), produced transmission failures at +/+ NMJs at high stimulus frequencies (Figure 7C) as well as decreased phosphorylation of MLC detected by immunostaining (Figure 7A, bottom right pair), demonstrating that Rho kinase can modulate the MLCK-MLC pathway at the NMJ. Microcystin-LR, a phosphatase inhibitor that will inhibit MLC-P (and possibly other phosphatases), prevented the failures in the NCAM 180 null NMJ. This result is consistent with an adequate level of MLC phosphorylation, which is a balance between phosphorylation by MLCK and dephosphorylation by MLC-P, as being a critical variable for maintaining adequate transmission. However, inhibition of Rho kinase must affect a pathway in addition to the KEN ESKA-MLCK-MLC pathway, since application of both the KENESKA peptide and the Rho kinase inhibitor Y-27632 (Figure 7, bar graph) produced a number of failures that was approximately the sum of that produced by Y-27632 (Figure 7, bar graph) or KENESKA (Figure 3B, left) alone.

In summary, these data make a strong case for a pathway in which the KENESKA domain of NCAM mediates the activation of MLCK. This in turn regulates MLC, which is required for effective transmission at high stimulus rates. We speculate that one of the nonmuscle myosins is the downstream target of this pathway and that it may act either by facilitating the delivery of vesicles to active zones or their subsequent exocytosis. Since myosin IIA and IIB are regulated by MLC and are present presynaptically, we assessed the effect of blebbistatin, which specifically inhibits nonmuscle myosin IIA and IIB, but not myosin Va, myosin X, or smooth muscle myosin II (Straight et al., 2003). Application of 100 μM blebbistatin produced approximately the same number and pattern of transmission failures at 100 Hz (Figure 8A) as had the phospho-KENESKA peptide (Figure 3B). This suggests that the effects of the KENESKA peptide are likely mediated by interfering with a myosin II-mediated process. The rescue of failures in the 180 null NMJ by the phosphatase inhibitor microcystin-LR also appears to be via myosin II, since the failures produced by blebbistatin in wild-type NMJs were not rescued by microcystin-LR (Figure 8B). However, when blebbistatin-treated NMJs were exposed to either the phospho-KENESKA peptide or the Rho kinase inhibitor, additional failures were produced. While the number of failures was less than the sum of those produced by blebblistatin and either of these agents alone, these results suggest that both the KENESKA and Rho kinase signaling pathways are likely to affect a process involved in maintaining effective transmission in addition to that mediated by mysosin II.

While the effects on transmission produced by the various peptides appeared to be presynaptic, bath application of the peptide-carrier complex should result in peptides entering both the presynaptic terminal and the muscle fiber. Thus we cannot exclude that some of the peptides produced presynaptic effects indirectly by first acting on muscle or Schwann cells (see, for example, Micheva et al., 2003). To provide more direct evidence for the site of action, a micropipette containing the phospho-KENESKA peptide-Chariot complex was positioned close to an endplate, based on the recording of extracellular synaptic currents (Polo-Parada et al., 2001). Applying current pulses for 30 min to eject the peptide-carrier complex (see Experimental Procedures) was sufficient to cause failures with 100 Hz nerve stimulation (Figure 8C), confirming that we were able to eject a sufficient amount of peptide by this method to cause a response. When the same delivery protocol was used to eject peptide synaptically after impaling a muscle fiber, no failures were produced. Taken together, this evidence indicates a presynaptic site of action for the phospho-KENESKA peptide. The immunostaining for phospho-MLC (Figure 7A), which the various applied peptides altered in ways consistent with their effects on transmission, also appeared to be presynaptic; the punctate staining along the axon and in the terminal was above the focal plane of the postsynaptic ACh receptors visualized by fluorescently tagged α-BTX and was in fact localized in the same focal plane as presynaptic vesicle markers. Thus it is likely that most of the effects of the peptides we have observed result from a presynaptic site of action.

Discussion

Previous studies from this laboratory discovered a role for NCAM, specifically its 180 kDa isoform, in maintain-

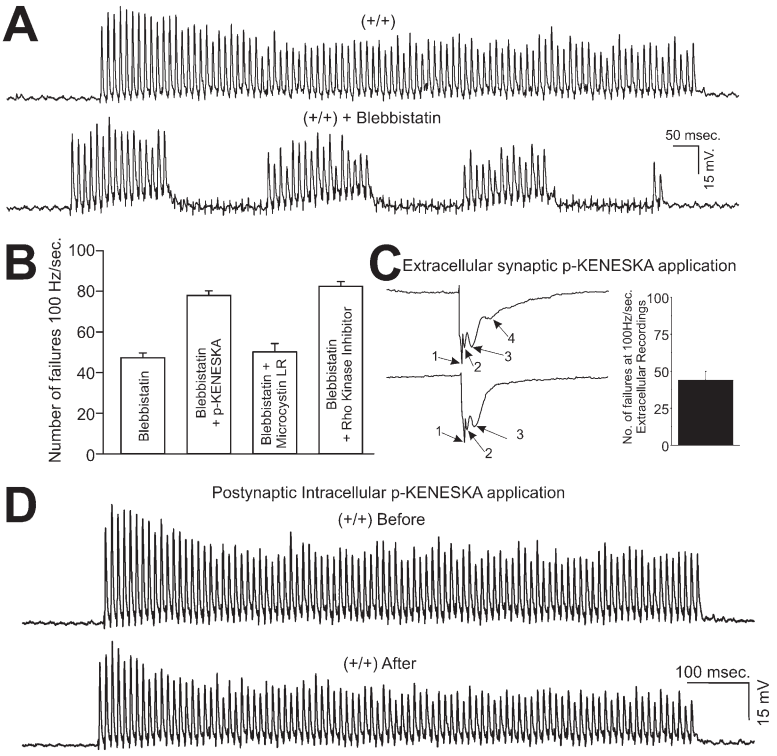

Figure 8. Transmission Failures Similar to Those Caused by Phospho-KENESKA Are Produced by the Myosin II Inhibitor Blebbistatin and a Presynaptic Site of Action Is Indicated for the Phospho-KENESKA Peptide

(A) Trains of EPPs at 100 Hz stimulation from the same cell prior to (top trace) and after (bottom trace) the application of 100 μM blebbistatin (recordings were made from superficial fibers, as blebbistain did not penetrate well into the muscle).

(B) Bar graph showing the number of failures/100 Hz train with blebbistatin alone or when blebbistatin was combined with either phospho-KENESKA, the phosphatase inhibitor Microcystin-LR (10 μM), or the Rho kinase inhibitor Y-27623 (100 μM).

(C) Extracellular iontophoresis of the phospho-KENESKA peptide resulted in failures during 100 Hz nerve stimulation; top trace, extracellular recording of synaptic current at start of train, showing stimulus artifact (1), presynaptic current (2 and 3), and postsynaptic current from EPP (4); bottom trace, a response from within the train where the postsynaptic response was missing. Bar graph, mean number of failures/100 Hz train.

(D) 100 Hz train of EPPs recorded postsynaptically from a muscle fiber before and after iontophoresis of the phospho-KENESKA peptide into the muscle fiber at the synaptic site. No failures occurred.

ing effective neuromuscular transmission with repetitive stimulation (Polo-Parada et al., 2001; Polo-Parada et al., 2004). We have now identified a highly conserved intracellular domain on NCAM that mediates these effects, and we provide substantial evidence that it acts by allowing sufficient MLCK activation; this in turn we speculate is required for myosin II-driven movements needed to replenish synaptic vesicles used during high-frequency stimulation. Introduction of the KEN ESKA peptide, which corresponds to the C-terminal portion of this conserved domain, into adult +/+ mouse NMJs produced transmission failures similar to those seen in the NCAM 180 null mouse. In contrast, this peptide had no effect on transmission in NMJs that lacked the 180 kDa NCAM isoform. The ability of NCAM to act as a signaling molecule has been increasingly appreciated (Crossin and Krushel, 2000; Hinsby et al., 2004), and the domain and pathway we describe here add to the expanding list of NCAM-mediated signaling pathways. In addition, since these effects were caused by acute application of the peptide in adult +/+ NMJs, the transmission defects seen in the 180 null mouse are unlikely to have resulted from developmental alterations caused by NCAM's absence; instead, our data point to the 180 isoform of NCAM as playing an essential role in adult neuromuscular transmission.

To elucidate the potential role of the KENESKA domain of NCAM in maintaining effective high-frequency transmission, we introduced this and other peptides directly into adult NMJs in acutely isolated muscles. We propose that the KENESKA peptide produced failures at +/+ NMJs by preventing this domain on synaptically localized 180 kDa NCAM from binding/interacting with other intracellular molecules required for the downstream activation of MLCK. The fact that the KENESKA peptide was without effect in NCAM 180 null NMJs and that a scrambled peptide or one in which the serine had been replaced with glycine was also without effect pointed to the specificity of these interactions and the importance of serine phosphorylation in regulating these effects of NCAM. The latter conclusion was strengthened by the fact that introduction of the serine phosphorylated KENESKA or one in which serine was replaced by an aspartate, mimicking a phosphorylated amino acid at this site, produced even more abundant transmission failures, closely approximating the 180 null phenotype. We suggest that the binding of this domain to an intracellular PDZ-like binding partner is regulated by phosphorylation of this serine.

Although both the 140 and 180 isoforms of NCAM possess the KENESKA domain, the 140 isoform was unable to compensate for the absence of the 180 isoform in preventing transmission failures. This could result if the 180 and 140 isoforms are located in different microdomains at the synapse, since the signaling pathways utilized by NCAM isoforms can depend on whether they are localized within lipid rafts (Niethammer et al., 2002). We have previously shown that the 180 isoform is localized presynaptically in a punctate pattern (Polo-Parada et al., 2004), but unfortunately, no antibody exists that allows one to determine the location of the 140 isoform. Alternatively, the KENESKA domain on the 140 isoform might be effectively masked, but the insertion of the alternatively spliced 180 unique

domain might allow the KENESKA domain to more effectively interact with its putative binding partners. In addition, a different localization of the 180 isoform might facilitate the phosphorylation of the serine within the KENESKA domain that would in turn mediate specific interactions of this isoform.

The transmission defects that have been described appear to be entirely presynaptic (Polo-Parada et al., 2001; Polo-Parada et al., 2004), and the effects of the peptides we have introduced are most likely explained by their acting presynaptically. We have not yet identified the protein that directly interacts with the KEN ESKA domain; however, the results of introducing peptides that either activated or inhibited MLCK alone or in combination with the KENESKA peptide clearly place this kinase at a critical position in the signaling pathway of the NCAM 180 isoform which prevents transmission failures. These observations confirm and extend several other studies showing the importance of MLCK in maintaining synaptic transmission in hippocampal (Ryan 1999) and sympathetic (Mochida et al., 1994; Mochida, 1995) neurons. The current study has also provided direct evidence that the KENESKA peptide and those that either inhibit or make MLCK constitutively active altered the phosphorylation of threonine18/serine 19 on MLC within in vivo NMJs in a manner consistent with MLCK's proposed role in transmission. This site on MLC is a main target of MLCK (Kamm and Stull 2001) that regulates the activation of myosins in smooth muscle, motile cells, neuronal growth cones, and secretory cells (Matsumura et al., 1998; Schmidt et al., 2002; Somlyo and Somlyo, 2003; Neco et al., 2004).

While we cannot be certain that the observed changes in phosphorylation of this site on MLC were responsible for the alterations in transmission produced by the various peptides alone or in combination, the data clearly indicate that introduction of the KEN ESKA peptide was able to bring about a biochemical change in MLC at this site consistent with the effects we observed on transmission. Taken together our data suggest that the ultimate downstream target of the KENESKA domain of NCAM in mediating effective transmission is likely to be one of the nonmuscle myosins, which have been implicated in either vesicle movement or synaptic transmission. Myosin Va, which we have shown is present at mouse NMJs, has been shown in several systems to couple synaptic vesicles with either actin filaments or microtubules and thus plays a role in their transport (Evans et al., 1998; Brown et al., 2003; Cao et al., 2004). However, hippocampal synapses of a mouse mutant for myosin Va exhibited normal transmission and plasticity (Schnell and Nicoll, 2001, but see Libby et al., 2004). In addition, our data on the effects of blebbistatin support instead a role for myosin II at mouse NMJs.

Myosin II is required to maintain normal transmission at sympathetic ganglion synapses (Mochida et al., 1994; Mochida, 1995) and for both the movement and subsequent exocytosis of vesicles in chromaffin cells (Neco et al., 2004; but see Rose et al., 2003). Our data, showing a pathway involving MLC, would be most consistent with a role for myosin II, where regulation by MLC is generally accepted. It would also fit nicely with studies by Mochida (Mochida et al., 1994; Mochida, 1995), which showed that interfering with the function of presynaptic myosin II at sympathetic ganglionic synapses produced a decline in transmission that was dependent on the synapses being activated. The fact that the decline in transmission depended on the pattern of stimulation and that the induction of PTP was also blocked led the authors to propose that myosin II was most likely involved in supplying vesicles to the active zone to replenish those released and thus was required to maintain transmission with repetitive stimulation. In our study as well, transmission failures only occurred at higher frequencies of stimulation and following a number of EPPs of normal amplitude.

The cycles of total transmission failures in both NCAM 180 null NMJs and +/+ NMJs treated with KEN ESKA peptides are unusual in that they imply an underlying process with some threshold that results in multiple release sites releasing either a normal amount of transmitter or none at all. This might occur if some threshold level of kinase activation was needed to engage a signaling pathway required to mobilize vesicles from the reserve pool. In its absence, no release sites would be replenished with synaptic vesicles. Some period of time, in the absence of exocytosis, might be required for this process to recover. Finally, it is clear that failures of exocytosis occur, but the extent to which alterations in either fast or slow forms of endocytic vesicle cycling (Virmani et al., 2003) contribute to the phenotype will require extensive characterization of cycling kinetics using styryl dyes, which is currently underway.

In summary, while more work will be needed to determine which myosins (myosin IIA or IIB) are involved in transmission at adult mouse NMJ as well as to elucidate their precise roles in synaptic vesicle movement and exocytosis required to maintain effective high-frequency transmission, it seems very likely that the pathway we have described involving the KENESKA domain of the 180 isoform of NCAM will play an essential role. The present study has also shown that it is possible to introduce peptides via a peptide carrier into the junctions of adult, acutely isolated muscles and that this method can be used to probe specific protein-protein interactions, including those regulated by the phosphorylation state of the protein. Such an approach should be widely useful in other isolated organ/tissue preparations.

Experimental Procedures

Mice

$Ncam^{tm1cwr}$ mice were generated by H. Tomasiewicz, as previously described (Polo-Parada et al., 2004). Wilde-type (+/+) and homozygous 180 knockout mice were identified by PCR using primers that distinguish wild-type from mutant alleles as described previously (Polo-Parada et al., 2001; Polo-Parada et al., 2004).

Electrical Recordings

Standard electrophysiological procedures were used to record from P30 acutely isolated semitendinosus muscles as described previously (Polo-Parada et al., 2001 and Polo-Parada et al., 2004). The semitendinosus muscle preparation was perfused with normal Tyrode's solution (125 mM NaCl, 5.37 mM KCl, 24 mM $NaHCO_3$, 1 mM $MgCl_2$, 1.8 mM $CaCl_2$, and 5% dextrose, containing 1 μM ω-conotoxin GIIIB) (Alomone Labs, Jerusalem, Israel), which spe-

cifically blocks voltage-gated sodium channels in muscle and thus contraction. Sharp glass electrodes were pulled (20–40 MΩ), filled with 3 M KCl, and single muscle fibers were impaled near the motor endplate. Potentials were recorded via intracellular amplifier (World Precision Instruments) using Axoscope software (40 KHz sampling rate; Axon Instruments, Union City, CA). The nerves were sucked into tight polyethylene-stimulating electrodes pulled from polyethylene tubing (PE-190; Clay Adams, Parsippany, NJ) and stimulated with a Grass SW38 stimulator thorough a PSIU6B isolation unit (Grass Instruments, Quincy, MA).

Perineural Recordings

Appropriate positioning of sharp electrodes close to the terminal allows electrotonically conducted currents from the nerve terminal to be recorded as voltage drops across the perinerium as previously described in detail (Brigant and Mallart, 1982; Urbano et al., 2002; Polo-Parada et al., 2004). Statitistical analyses were performed using Student's t test in Sigma plot 2.0.

Introduction of Peptides into Adult NMJs

Peptides were introduced into the semitendinosus NMJ-muscle preparation by using the Chariot protein method (Active Motif, Carlsbad, CA). Briefly a Chariot stock solution was prepared by diluting 1.2 mg of Chariot reagent in 600 μl ddH_2O and preserved at –70°C. The Chariot stock solution was further diluted to a final concentration of 2 μg in 100 μl of normal Tyrode's solution and sonicated in a water bath for 30 min. The peptides were prepared as a stock solution of 50 μM in ddH_2O and preserved at –70°C. An aliquot of 10 μl stock peptide solution was defrosted and further diluted to a final concentration of 15 μM in 100 μl of normal Tyrode's solution and sonicated for 30 min in a water bath. These two solutions were mixed, vortexed, and sonicated in a water bath for 1 hr to allow the Chariot-peptide complex to form. The Chariot/peptide complex mixture was then diluted to a final volume of 1 ml with normal Tyrode's solution, (final peptide concentration ~3 μM) and bubbled with 95%O_2/5% CO_2. The semitendinosus preparation was incubated in this mixture for 1 hr and then washed five times with normal Tyrode's solution and incubated for an additional 1 hr in the presence of oxygenated Tyrode's solution with 95%O_2/5%CO_2 containing 1 μM ω-conotoxin GIIIB. Then the preparation was washed five times with normal Tyrode's solution and continuously perfused with freshly oxygenated Tyrode's solution (0.2 ml/min) during recordings. To distinguish whether the phospho-KENESKA peptide was acting pre- or postsynaptically, a 50× Chariot-phospho-KENESKA complex was prepared as described above and diluted in 1 ml of 3 M KCl. Sharp electrodes were backfilled with this solution, and endplates were located by extracellularly recorded EPPs (see Polo-Parada et al., 2001). 5 ms pulses of 10 nA current were then injected into the pipette at a frequency of 10 Hz for 30 min to iontophorese the peptide complex onto the synaptic terminal. Following a 1 hr wash, the nerve was stimulated at 100 Hz, and the number of failures was determined by the loss of the postsynaptic component of the extracellular current recordings (see Polo-Parada et al., 2001). In other preparations, after detection of the extracellular EPP, the muscle fiber was impaled, the same protocol used to eject the phospho-KENESKA peptide, and the number of transmission failures determined.

Peptides used were as follows: the series used to probe the C-terminal domain of NCAM were KENESKA, KENE[p-Ser]KA, KENEGKA, KENEDKA, and CSNKATAETKQE. The MLCK-inhibitory peptide used is an 11-residue synthetic peptide analog, corresponding to part of the calmodulin binding sequence in skeletal muscle myosin light chain kinase. This peptide, LRRWLLNFIAV (Sigma, Saint Louis, MO), inhibited calmodulin-dependent activation of the smooth muscle myosin light chain kinase (Kemp et al., 1987). The MLCK agonist peptide sequence was SKDRMKKYMA (from the 788 to 796 aa of the inhibitory domain of MLCK; Tanaka et al., 1995). The MLC inhibitory peptide had the sequence KQAQRGSSNVFSM and was derived from sequences flanking the serine 19/threonine 18 on MLC (Swiss Prot |Q9QVP4|MLRA_Mouse) that are phosphorylated by MLCK and mimic the MLC-substrate. The peptides were 95% pure and synthesized by the Analysis Dept., Wolfson Institute for Biomedical Research, London.

Immunostaining

P30 mice were sacrificed in CO_2 chamber, and semitendinosus muscles were quickly removed and fixed in 3.7% formaldehyde, 5% sucrose in PBS and cryoprotected in 30% sucrose overnight. Frozen sections (30 μM) were cut, air-dried, and stored at –70°C. All stainings were performed by blocking the sections with 2% BSA in PBS and incubation with the appropriate primary antibodies at 4°C for 24 hr, followed by incubations with fluorochorome-conjugated secondary antibodies (Zymed, San Francisco, CA). Primary antibodies used were pMLC2 (T18/S19), from Cell Signaling Technology (Beverly, MA), and myosin IIA, IIB, and Va from Sigma (St. Louis, MO). Pictures were acquired and processed with an Olympus Magnifier CCD camera or a Olympus 2000 camera (Olympus, America) and Adobe Photoshop 8.0, respectively. Quantification of immunostaining was as described in Polo-Parada et al., 2004.

SDS-PAGE Immunobloting

PC12 cells were grown to 95% confluence in DMEM + 10% FBS in a 10% CO_2 incubator. PC12 cells were exposed to 55 mM KCl for 1 min, washed five times with standard Tyrode's solution, and after a 5 min delay, lysates were prepared from unstimulated or K^+-stimulated cultures. In two additional sister cultures, the Chariot method was used to introduce the caMLCK peptide into the cells as described previously. One culture was unstimulated while the other was exposed to the same KCl protocol previously described. Cells were homogenized in HEPES extraction buffer (25 mM HEPES, 150 mM NaCl, 1 mM EDTA) containing 1% NP-40 and protease inhibitor mixture (Roche Diagnostics, Manheim, Germany). The solubilized protein concentration was determined (BCA method; Pierce, Rockford, IL) and adjusted to 1 μg/ml. SDS sample buffer containing dithiotheritol was added to each sample, and the proteins were separated by SDS-page according to the Laemmli method on a 20% gel. The proteins were transferred onto polyvinylidene fluoride membranes, which were immunostained with a phospho-myosin light chain (Thr18/Ser19) antibody (Cell Signaling, Beverly MA) and appropriate HRP-conjugated secondary antibody, which was visualized with a chemiluminescence kit (ECL, Pierce). Quantification of the MLC band was performed using the Versidoc gel quantification system.

Bioinformatics

Conserved regions within the intracellular domain of NCAM 180 (SWISS PROT|P13595|NCA1_MOUSE) were detected with the sequence alignment program ClustalW (Thompson et al., 1994). Conserved sequences were searched for homologies with P-Blast (Altschuh et al., 1997). Secondary structure was predicted using the software PHDsec (Rost and Sander, 2000), and potential phosphorylation sites were detected using NetPhos (Blom et al., 1999).

Acknowledgments

We thank Susann Brady-Kalnay, Thomas Egelhoff, Gary Landreth, Sumiko Mochida, and Stefan Herlitze for helpful discussions of the experiments and comments on the manuscript. Special thanks to Katherine Lobur for her excellent care of the mice and to Gary Landreth and Allison Limpert for providing the PC12 cells used in the biochemical experiments. Supported by NIH grants NS23678 and NS19640 from NINDS and an AHA grant 0530140N to L.P.-P.

Received: December 14, 2004
Revised: April 1, 2005
Accepted: May 6, 2005
Published: June 15, 2005

References

Altschuh, S.F., Madden, T.L., Schaffer, A.A., Zhang, J., Zhang, Z., Miller, W., and Lipman, D.J. (1997). Gapped BLAST and PSI-BLAST: a new generation of protein database search programs. Nucleic Acids Res. *25*, 3389–3402.

Barbas, J.A., Chaix, J.C., Steinmetz, M., and Goridis, C. (1988). Differential splicing and alternative polyadenylation generates distinct NCAM transcripts and proteins in the mouse. EMBO J. *7*, 625–632.

Blom, N., Gammeltoft, S., and Brunak, S. (1999). Sequence- and structure-based prediction of eukaryotic protein phosphorylation sites. J. Mol. Biol. *294*, 1351–1362.

Brigant, J.L., and Mallart, A. (1982). Presynaptic currents in mouse motor endings. J. Physiol. *333*, 619–636.

Brown, M.E., and Bridgman, P.C. (2003). Myosin function in nervous and sensory systems. J. Neurobiol. *58*, 118–130.

Brown, J.R., Stafford, P., and Langford, G.M. (2003). Short-range axonal/dendritic transport by myosin-V; a model for vesicle delivery to the synapse. J. Neurobiol. *58*, 175–188.

Buttner, B., Kannicht, C., Reutter, W., and Horstkorte, R. (2003). The neural cell adhesion molecule is associated with major components of the cytoskeleton. Biochem. Biophys. Res. Commun. *310*, 967–971.

Cao, T.T., Chang, W., Masters, S.E., and Mooseker, M.S. (2004). Myosin-Va binds to and mechanochemically couples microtubules to actin filaments. Mol. Bio. Cell *15*, 151–161.

Chung, H.J., Huang, Y.H., Lau, L.-T., and Huganir, R.L. (2004). Regulation of the NMDA receptor complex and trafficking by activity-dependent phosphorylation of the NR2B subunit PDZ ligand. J. Neurosci. *24*, 10248–10259.

Craven, S.E., and Bredt, D.S. (1998). PDZ proteins organize synaptic signaling pathways. Cell *93*, 495–498.

Crossin, K.L., and Krushel, L. (2000). Cellular signaling by neural cell adhesion molecules of the immunoglobulin superfamily. Dev. Dyn. *218*, 260–279.

Cunningham, B.A., Hemperly, J.J., Murray, B.A., Prediger, E.A., and Edelman, G.M. (1987). Neural cell adhesion molecules: structure, immunoglobulin-like domains, cell surface modulation and alternative splicing. Science *236*, 799–806.

Evans, L.L., Lee, A.J., Bridgman, P.C., and Mooseker, M.S. (1998). Vesicle-associated brain myosin-V can be activated to catalyze actin-based transport. J. Cell Sci. *111*, 2055–2066.

Hinsby, A.M., Berezin, V., and Bock, E. (2004). Molecular mechanisms of NCAM function. Front. Biosci. *9*, 2227–2244.

Isotani, E., Zhi, G., Lau, K.S., Huang, J., Mizuno, Y., Persechini, A., Geguchadze, R., Kamm, K.E., and Stull, J.T. (2004). Real-time evaluation of myosin light chain kinase activation in smooth muscle tissues from a transgenic calmodulin-biosensor mouse. Proc. Natl. Acad. Sci. USA *101*, 6279–6284.

Kabouridis, P.S. (2003). Biological applications of protein transduction technology. Trends Biotechnol. *21*, 498–503.

Kamm, K.E., and Stull, J.T. (2001). Dedicated myosin light chain kinases with diverse cellular functions. J. Biol. Chem. *276*, 4527–4530.

Kay, B.K., Williamson, M.P., and Sudol, M. (2000). The importance of being proline: the interaction of proline-rich motifs in signaling proteins with their cognate domains. FASEB J. *14*, 231–241.

Kemp, B.E., Pearson, R.B., Guerriero, V., Bagchi, I., and Means, A.R. (1987). The calmodulin binding domain of chicken smooth muscle myosin light chain kinase contains a psuedosubstrate sequence. J. Biol. Chem. *262*, 2542–2548.

Kim, E., and Sheng, M. (2004). PDZ domain proteins of synapses. Nat. Rev. Neurosci. *5*, 771–781.

Kiss, J.Z., and Muller, D. (2001). Contribution of the neural cell adhesion molecule to neuronal and synaptic plasticity. Rev. Neurosci. *12*, 297–310.

Kolkova, K., Novitskaya, V., Pederson, N., Berezin, V., and Bock, E. (2001). Neural cell adhesion molecule-stimulated neurite outgrowth depends on activation of protein kinase C and the Ras-mitogen activated protein kinase pathway. J. Neurosci. *20*, 2238–2246.

Libby, R.T., Lillo, C., Kitamoto, J., Williams, D.S., and Steel, K.P. (2004). Myosin Va is required for normal photoreceptor synaptic activity. J. Cell Sci. *117*, 4509–4515.

Matsumura, F., Ono, S., Yamakita, Y., Totsukawa, G., and Yamashiro, S. (1998). Specific localization of serine 19 phosphorylated myosin II during cell locomotion and mitosis of cultured cells. J. Cell Biol. *140*, 119–129.

Micheva, K.D., Buchanan, J., Holz, R.W., and Smith, S.J. (2003). Retrograde regulation of synaptic vesicle endocytosis and recycling. Nat. Neurosci. *6*, 925–932.

Mochida, S. (1995). Role of myosin in neurotransmitter release: functional studies at synapses formed in culture. J. Physiol. (Paris) *89*, 83–94.

Mochida, S., Kobayashi, H., Matsuda, Y., Yuda, Y., Muramoto, K., and Nonomura, Y. (1994). Myosin II is involved in transmitter release at synapses formed between rat sympathetic neurons in culture. Neuron *13*, 1131–1142.

Neco, P., Giner, D., Viniegra, S., Borges, R., Villarroel, A., and Gutierrez, L.M. (2004). New roles of myosin II during vesicle transport and fusion in chromaffin cells. J. Biol. Chem. *279*, 27450–27457.

Niethammer, P., Delling, M., Sytnyk, V., Dityatev, A., Fukami, K., and Schachner, M. (2002). Cosignaling of NCAM via lipid rafts and the FGF receptor is required for neuritogenesis. J. Cell Biol. *157*, 521–532.

Panicker, A.K., Buhusi, M., Thelen, K., and Maness, P.F. (2003). Cellular Signaling mechanisms of neural cell adhesion molecules. Front. Biosci. *8*, 900–911.

Polo-Parada, L., Bose, C.M., and Landmesser, L.T. (2001). Alterations in transmission, synaptic vesicle dynamics, and the organization of transmitter release machinery at N-CAM deficient neuromuscular junctions. Neuron *32*, 815–828.

Polo-Parada, L., Bose, C.M., Plattner, F., and Landmesser, L.T. (2004). Distinct roles of different neural cell adhesion molecule (NCAM) isoforms in synaptic maturation revealed by analysis of NCAM 180 kDa isoform-deficient mice. J. Neurosci. *24*, 1852–1864.

Riento, K., and Ridley, A.J. (2003). ROCKs: Multifunctional kinases in cell behavior. Nat. Rev. Mol. Cell. Bio. *4*, 446–456.

Rose, S.D., Lejen, T., Larson, R.E., Pene, T.D., and Trifaro, J.M. (2003). Myosins II and V in chromaffin cells: myosin V is a chromaffin vesicle molecular motor involved in secretion. J. Neurochem. *85*, 287–298.

Rost, B., and Sander, C. (2000). Third generation prediction of secondary structures. Methods Mol. Biol. *143*, 71–95.

Rutishauser, U., and Landmesser, L. (1996). Polysialic acid in the vertebrate nervous system: a promoter of plasticity in cell-cell interactions. Trends Neurosci. *19*, 422–427.

Ryan, T.A. (1999). Inhibitors of myosin light chain kinase block synaptic vesicle pool mobilization during action potential firing. J. Neurosci. *19*, 1317–1323.

Safell, J.L., Williams, E.J., Mason, I.J., Walsh, F.S., and Doherty, P. (1997). Expression of a dominant negative FGF receptor inhibits axonal growth and FGF receptor phosphorylation stimulated by CAMs. Neuron *18*, 231–242.

Sanes, J.R., and Lichtman, J.W. (1999). Development of the vertebrate neuromuscular junction. Annu. Rev. Neurosci. *22*, 389–442.

Schmid, R.S., Graff, R.D., Schaller, M.D., Chen, S., Schachner, M., Hemperly, J.J., and Maness, P.F. (1999). N-CAM stimulates the Ras-MAPK pathway and CREB phosphorylation in neuronal cells. J. Neurobiol. *38*, 542–558.

Schmidt, J.T., Morgan, P., and Leu, B. (2002). Myosin light chain phosphorylation and growth cone motility. J. Neurobiol. *52*, 175–188.

Schnell, E., and Nicoll, R. (2001). Hippocampal synaptic transmission and plasticity are preserved in myosin Va mutant mice. J. Neurophysiol. *85*, 1498–1501.

Somlyo, A.P., and Somlyo, A.V. (2003). Ca^{2+} sensitivity of smooth muscle and nonmuscle myosin II: modulated by G proteins, kinases, and myosin phosphatase. Physiol. Rev. *83*, 1325–1358.

Straight, A.F., Cheung, A., Limouze, J., Chen, I., Westwood, N.J., Sellers, J.R., and Mitchison, T.J. (2003). Dissecting temporal and spatial control of cytokinesis with a myosin II inhibitor. Science *14*, 1743–1747.

Tanaka, M., Ikebe, R., Matsuura, M., and Ikebe, M. (1995). Pseudosubstrate sequence may not be critical for autoinhibition of smooth muscle myosin light chain kinase. EMBO J. *14*, 2839–2846.

Thompson, J.D., Higgins, D.G., and Gibson, T.J. (1994). ClustalW:

improving the sensitivity of progressive multiple sequence alignment through sequence weighting, position-specific gap penalties and weight matrix choice. Nucleic Acids Res. *22*, 4673–4680.

Urbano, F.J., Rosata-Siri, M.D., and Uchitel, O.D. (2002). Calcium chanels involved in neurotransmitter release at adult, neonatal and P/Q-type deficient neuromuscular junctions. Mol. Membr. Biol. *19*, 293–300.

Virmani, T., Han, W., Liu, X., Sudhof, T.C., and Kavalali, E.T. (2003). Synaptotagmin 7 splice variants differentially regulate synaptic vesicle cycling. EMBO J. *22*, 5347–5357.

Wahl, S., Barth, H., Ciossek, T., Aktories, K., and Mueller, B.K. (2000). Ephrin-A5 induces collapse of growth cones by activating Rho and Rho kinase. J. Cell Biol. *149*, 263–270.